1085-9195/98/29/225–241/$12.25

Cell Contraction Caused by Microtubule Disruption Is Accompanied by Shape Changes and an Increased Elasticity Measured by Scanning Acoustic Microscopy

*Ilonka Karl and Jürgen Bereiter-Hahn**

Cinematic Cell Research Group, Department of Zoology, Johann Wolfgang Goethe University, Biocenter, Marie-Curie-Str. 9, D 60439 Frankfurt am Main, Germany;
E-mail: bereiter-hahn@zoology.uni-frankfurt.de

ABSTRACT

The state of crosslinking of microfilaments and the state of myosin-driven contraction are the main determinants of the mechanical properties of the cell cortex underneath the membrane, which is significant for the mechanism of shaping cells. Therefore, any change in the contractile state of the actomyosin network would alter the mechanical properties and finally result in shape changes. The relationship of microtubules to the mechanical properties of cells is still obscure. The main problem arises because disruption of microtubules enhances acto-myosin-driven contraction. This reaction and its impact on cell shape and elasticity have been investigated in single XTH-2 cells. Microtubule disruption was induced by colcemid, a polymerization inhibitor. The reaction was biphasic: a change in cell shape from a fried egg shape to a convex surface topography was accompanied by an increase in elastic stiffness of the cytoplasm, measured as longitudinal sound

*Author to whom all correspondence and reprint requests should be addressed.

velocity revealed by scanning acoustic microscope. Elasticity increases in the cell periphery and reaches its peak after 30 min. Subsequently while the cytoplasm retracts from the periphery, longitudinal sound velocity (elasticity) decreases. Simultaneously, a two- to threefold increase of F-actin and alignment of stress fibers from the cell center to cell–cell junctions in dense cultures are induced, supposedly a consequence of the increased tension.

Index Entries: Microtubules; cell shape; cytomechanics; cytoskeleton; F-actin; elasticity; mechanical properties; acoustic microscopy.

INTRODUCTION

The mechanical properties of the cell cortex are considered to be of crucial significance for the shape of a cell and its motile behavior. Actin fibers participate to a large extent in these mechanisms because their organization — e.g., the state of crosslinking and the state of myosin-driven contraction — is the main determinant of the mechanical properties of the cell cortex underneath the membrane *(1,2)*. The cortical fibrillar network generates an intracellular hydrostatic pressure *(3,4)*, which, in combination with the adhesion to the substratum, and cellular organelles and local stiffness differences in the cortex, is proposed to shape a cell. Therefore, any change in the contractile state of the actomyosin network would alter the mechanical properties and finally result in shape changes.

Microtubule disruption is supposed to change the contractile state of cells: inhibitors of polymerization induce contraction in tissue culture cells *(5)*. Disregarding the unknown signal transduction pathway of the phenomena, the disruption of microtubules was found to be associated with increased phosphorylation of the myosin regulatory light chain *(6)*, which is the usual control mechanism underlying actomyosin-driven contractility in nonmuscle cells.

Measurements of the mechanical properties related to a given cell shape and to cytoskeletal organization of living cells have been achieved for different cell types by scanning acoustic microscopy (SAM) *(7,8)*. Images recorded by SAM provide information about cell topography and the elastic properties of cells with high lateral resolution *(9,10)*.

The aim of the present report was to determine subcellular elasticity modulations during disassembly of microtubules using SAM.

Microtubule disassembly was favored by colcemid, an inhibitor of tubulin polymerization. XTH-2 cells a cell line derived from *Xenopus laevis* tadpole heart endothelia *(11)*, exhibit a dome-shaped cell center and a flat periphery. In parallel with changes in cytoplasmic elasticity, dramatic alterations of shape were observed during colcemid treatment by reflection interference contrast microscopy (RIC). In addition, the F-actin content increases during contraction stimulated by microtubule disruption.

MATERIALS AND METHODS

Cell Culture

XTH-2 cells were cultured at 28°C in minimum essential medium (MEM) with Eagle's salts supplemented with 10 m*M* HEPES, 1% penicillin streptomycin neomycin (PSN), 0.2% $NaHCO_3$ and 5% fetal calf serum (FCS; all from GIBCO, Glasgow, UK) and split 1:3 twice a week. For experiments, the trypsinized cells were plated on glass cover slips in Petri dishes with 2 mL of cell suspension each. Cells were used for experiments 2–3 d after plating with a cell density of 100–150 cells/mm^2.

Colcemid Treatment

Stock solution of colcemid (Demecolcine; Sigma, Deisenhofen, Germany) was prepared in distilled water (1 mg/mL), stored at 4°C, and added to cell cultures to a final concentration of 10^{-5} *M*.

Immunofluorescence

For immunolabeling of microtubules, cells grown on glass cover slips were fixed in methanol (–20°C) for 10 min, washed in phosphate-buffered saline (PBS), incubated at room temperature for 30 min with monoclonal antibodies against either tyrosinated (YL½) or detyrosinated (ID5) α-tubulin *(12)* (kindly provided by J. Wehland, Bochum, Germany), washed in Ca^{2+}/Mg^{2+}-free PBS, and incubated with either fluorescein isothiocyanate (FITC)-conjugated antirat (Sigma) or tetrarhodamine isothiocyanate (TRITC)-conjugated antimouse (Boehringer-Mannheim, Mannheim, Germany) antibody. For TRITC-phalloidin labeling of F-actin *(13)*, cells grown on glass cover slips were fixed at room temperature for 20 min in 5% formaldehyde in Ca^{2+}/Mg^{2+}-free PBS, washed, and incubated at room tem-

perature with TRITC-conjugated phalloidin (0.175 μg/100 μL). After staining, the cover glasses were rinsed repeatedly with PBS and mounted onto slides in ProLong™ mounting medium (Molecular Probes Europe BV, Leiden, The Netherlands). Fluorescence microscopy was done using a confocal laser scanning microscope (TCS, Leica, Wetzlar, Germany) with a ×63 oil immersion objective.

Microfluorometry

The fluorescence of TRITC-phalloidin-labeled F-actin was measured using an Axiovert 35 microscope (Zeiss, Oberkochen, Germany) equipped with a photomultiplier and a scanning stage *(14)*. The specimen was mounted on a scanning stage and scanned along several lines using a ×63 oil immersion objective and a circular diaphragm with a virtual diameter of 25 μm. About 500 fields were measured per slide, and the data were stored in a PC, which also controlled the scanning movement of the microscope stage (Merzhäuser, Giessen, Germany). The mean of the line scans was calculated with consideration to the cell density and is expressed as relative F-actin content in arbitrary units.

Reflection Interference Contrast Video Microscopy (RIC)

The cell shape of XTH-2 cells during colcemid treatment was observed at room temperature using an RIC microscope (Diavert, Leitz, Wetzlar, Germany; for a description of the method, *see* ref. *15*) with a ×100 oil immersion objective and recorded on video tape using a Proxitronic intensified charge-coupled device (CCD) camera (Proxitronic, Bensheim, Germany) and the image processor Argus 20 (Hamamatsu, Hershing, Germany).

Scanning Acoustic Microscopy (SAM)

An ELSAM (Leica, Wetzlar, Germany) operated at a frequency of 1.0 GHz at room temperature was used, equipped with a lens with a radius of 40 μm and an opening angle of 100°. The interference pattern was used to analyze the distribution of stiffness based on the contrast among the interference fringes. The fringes result from the interference of sound waves reflected from the surface of the substratum and the medium-facing surface of the cells, respectively. Contrast differences in the interference pattern reflect variations in the acoustic impedance *(16)*, which is a product of density and sound

velocity. Variations in acoustic impedance of the cortical cytoplasm are revealed by the reflectivity of the cells, thus showing variations in subcellular stiffness distribution: Sound velocity *(c)* is proportional to the modulus of elasticity *(E)* and to the density of the material (ρ) where propagation takes place as described by the following equation:

$$c^2 = E/\rho$$

In fluids and gases, the compression modulus is the appropriate modulus of elasticity. In solid bodies, with limited lateral extension, *E* is Young's modulus. The shear modulus determines propagation of shear waves. Both tension and pressure are expressed as force per unit area, as is *E*. In the present contribution, Young's modulus was used as the appropriate determinant of longitudinal sound-wave velocity in cytoplasm. This interpretation is based on a physical model of cytoplasm assuming biphasic organization: The fibrillar elements of cytoplasm are considered as quasi-solids that exhibit spring-like elasticity, embedded in a fluid phase containing the soluble composites of a cell.

Model calculations on the amplitude of sound waves resulting from the interference of sound reflected at the upper surface of a wedge-shaped thin layer with its lower surface attached to glass clearly show that the resulting intensity variations in the interferences resulting from thickness changes along the wedge increase with increasing differences of acoustic impedance. This principle can be used for quantitative measurement of sound velocity corresponding to stiffness of the cytoplasm of cells in culture *(17)*.

Following the method of Litniewski and Bereiter-Hahn *(17)*, the sound velocity was evaluated. Images of cells attached to glass slides were taken with a focus 9–12 μm above the surface of the substratum. The acoustical parameters of the glass substratum used for calculations were: longitudinal sound velocity 5.87 km/s and density 2472 kg/m^3. The sound velocity of the culture medium was assumed to be 1.51 km/s. Density of the cytoplasm was assumed to be constant throughout the cell and equal to 1060 kg/m^3. The error of sound velocity calculations is reduced to 13–20 m/s, because of averaging the images.

Evaluation of Cell Volume

Images of cells attached to plastic were taken by SAM in focus on the surface of the substratum ($z = 0$) during colcemid treatment at

t = 0 and 60 min. The volume was evaluated using a Quantimet (Leitz) by summing up the area surrounded by each interference fringe multiplied with its thickness, a quarter of the wavelength (l = 590 nm), following the method described by Hegner and Bereiter-Hahn *(18)*.

RESULTS

Effect of Colcemid Treatment on Microtubules

Microtubules were visualized by indirect immunofluorescence with monoclonal antibodies directed against two different posttranslationally modified types of α-tubulin: YL $^1/_2$ against tyrosinated tubulin and ID5 for detyrosinated tubulin. Microtubules containing mainly detyrosinated tubulin are assumed to be more stable *(19)*.

In untreated subconfluent XTH-2 cells, all microtubules seem to originate from a microtubule organizing center located above the nucleus, and they extend into the flat cell periphery. The microtubules detected with YL½ are rectilinear or slightly curved at their ends, turning parallel to the edge of the cell (Fig. 1A). Fewer microtubules were detected with the monoclonal antibody ID5. ID5-positive microtubules appear curved (Fig. 1D). After 30 min of colcemid treatment, the microtubules detected by YL $^1/_2$ no longer reach the cell margins, and they are less regular (Fig. 1B). At this time, the physiological function of microtubules can be assumed to be disturbed. One hour of colcemid incubation totally destroys the microtubules detected by YL½ (Fig 1C), whereas microtubules detected by ID5 were less affected (Fig. 1F), probably because of their slower turnover *(19)*.

Effect of Colcemid Treatment on F-Actin

To study the interaction between microtubules and actin fibers, the influence of microtubule disruption on F-actin content and the organization of F-actin was examined (Fig. 2). The relative F-actin content of XTH-2 cells was determined fluorometrically after colcemid or taxol treatment and after incubation at low temperature (4°C; Fig. 3). Colcemid induces the development of thicker stress fibers in confluent cells as well as in sparse cultures. After 60 min of colcemid treatment, in confluent layers, cells retract from some points of intercellular contact. Stress fibers become focused from the cell center to the remaining cell–cell junctions (Fig. 2B). After 1 h in colcemid or low

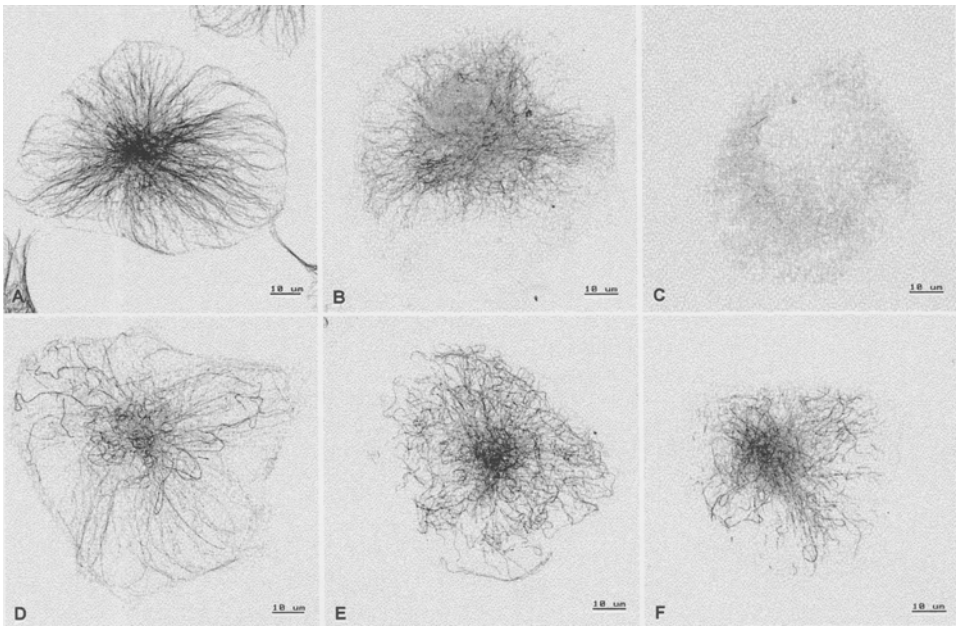

Fig. 1. Colcemid-induced disassembly of microtubules in single XTH-2 cells. Indirect immunofluorescence staining by the first monoclonal antibodies: YL $^1/_2$ against tyrosinated tubulin **(A–C)** and ID5 against detyrosinated tubulin **(D–F)**. (A–C) Untreated single XTH-2 cells (A) after 30 min of colcemid treatment (B), and after 60 min of colcemid treatment (C). After 30 min of incubation with colcemid the microtubules are less regular and shorter, i.e., most of the microtubules do not extend into the cell periphery. After 60 min there are only short fibrillar elements. (D–F) Microtubules stained with ID5 in an untreated XTH-2 cell (D), after 30 min of colcemid treatment (E), and after 60 min of colcemid treatment (F). The microtubules containing detyrosinated tubulin are diminished and appear wavy and fragmented.

temperature (4°C), the F-actin content increased to more than twice that of untreated cells. Taxol, which stabilizes microtubules *(20)*, had no effect on the F-actin content (Fig. 3).

Colcemid-Induced Shape Changes

Using an appropriate angle of illumination, RIC visualizes the surface topography of a cell: Light reflected from the substratum interferes with waves reflected from the medium-facing surface of the cell; the resulting interference fringes delineate surface topogra-

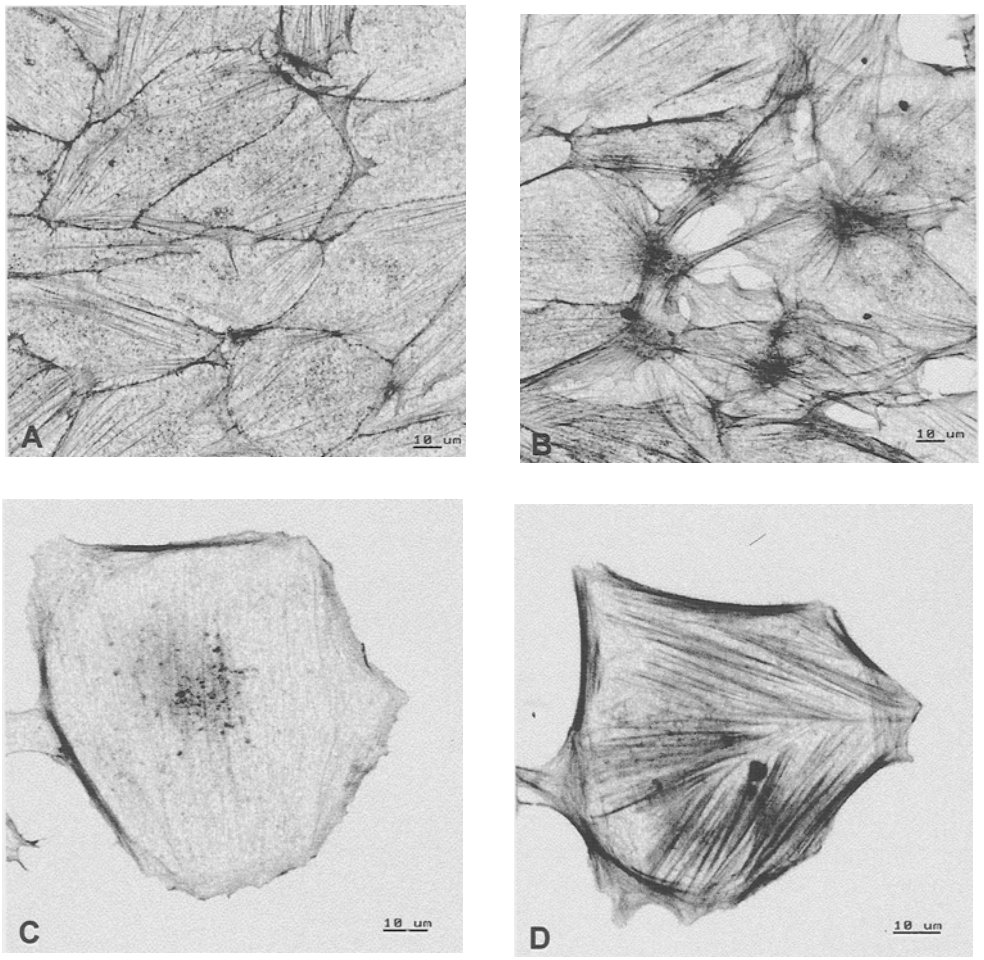

Fig. 2. Colcemid-induced F-actin changes in XTH-2 cells shown by TRITC-phalloidin staining. **(A,B)** Confluent culture untreated (A) and after 60 min of colcemid treatment (B). Colcemid induces the formation of stress fibers. Some cells are obviously retracted and only connected to each other via cytoplasmic threads. In several cells the stress fibers are focused at some points. **(C,D)** A single untreated XTH-2 cell (C) and after 60 min of colcemid treatment (D). The stress fibers are thicker than in controls.

phy (Fig. 4A). During colcemid treatment, the interference fringes first displace toward the cell periphery (Fig. 4B,C). This means that the cell flattens in the cell center and cytoplasm flows into the thickening periphery. Subsequently, with a temporal delay of approximately 20–30 min, the peripheral cytoplasm of the cell retreats,

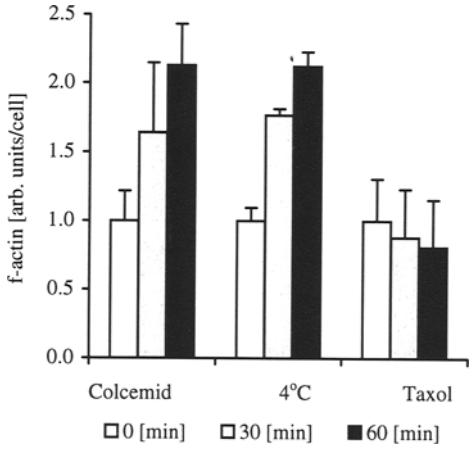

Fig. 3. F-actin content of XTH-2 cells during different microtubule-influencing conditions. XTH-2 cells were incubated with 10^{-5} *M* colcemid, taxol, or low temperature for 30 and 60 min, fixed, and stained with TRITC-phalloidin; the fluorescence was measured by microfluorometry. Disassembly of microtubules with colcemid or low temperature induces an increase of F-actin content after 30 and 60 min more than double that of untreated cells. The differences are significant at the $p < 0.05$ level. Incubation with taxol has no effect on f-actin content.

whereas some thin patches of cytoplasm and some retraction fibers remain (Fig. 4D). The cell volume does not change during this process (Fig. 5). No such changes in cell shape take place in human keratinocytes (HaCat). Their normal shape resembles that of XTH-2 cell after colcemid treatment.

Stiffness Changes on Microtubule Disassembly

The square of the longitudinal sound velocity of cells is linearly related to their elastic stiffness. During colcemid treatment (Fig. 6A, B), the sound velocity of cells ($n = 6$) increases by about 10–20% in the area of the first- and second-order interference fringes (corresponding to the thin peripheral cytoplasmic layer; Fig. 6C). After 30 min of colcemid treatment, sound velocity reaches a maximum. Thus the stiffening does not exceed a certain maximum value (around 1.9 km/s, corresponding to about $2.7 \times 10^3/\mathrm{Nm}^2$). After 60 min the sound velocity in the periphery is decreased but still higher than in untreated cells.

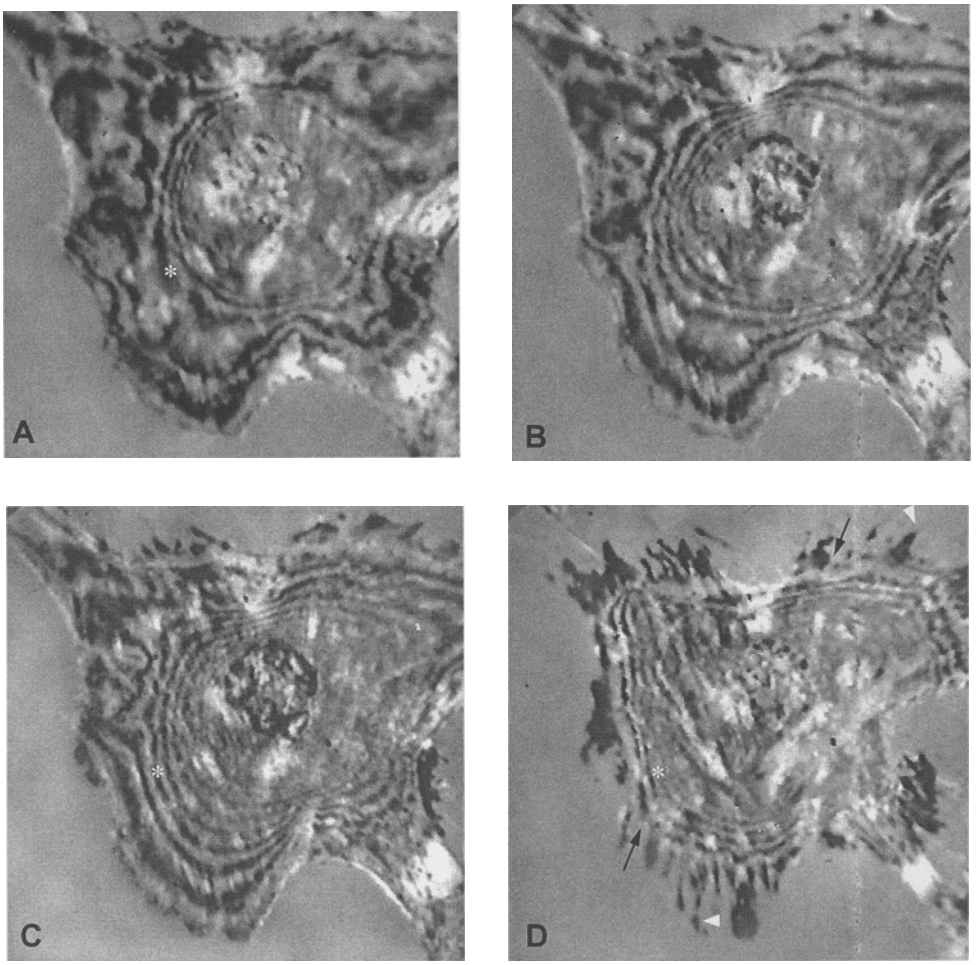

Fig. 4. Shape changes of a single XTH-2 cell during colcemid treatment (10^{-5} *M*) as revealed by RIC. The distribution of interference fringes visualizes the surface topography of the cell. **(A)** The untreated cell shows the typical fried egg shape, with the dome-shaped cell center with a high slope (delineated by the almost circular interference fringes) and the flat periphery (broad interference fringes). **(B,C)** After 10 min (B) and 20 min (C) of colcemid treatment, the interference fringes become displaced toward the cell periphery. In A, C, and D, the asterisk indicates the corresponding interference fringe that marks zones of the same thickness, assuming the refractive index of cytoplasm remains constant. The cell flattens in the cell center and becomes thicker in the periphery, resulting in a convex cell shape. **(D)** After 60 min, the peripheral cytoplasm at the cell edge is retracted (black arrows). Only thin cytoplasmic layers and some retraction fibers remain, appearing black because they are closely attached to the substratum (white arrowheads).

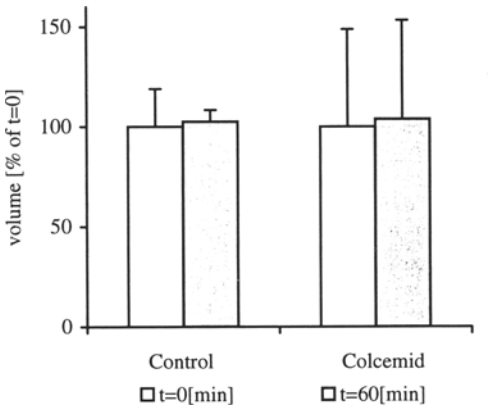

Fig. 5. Volume of XTH-2 cells (n = 10) before and after 60 min of colcemid treatment. The data were derived from SAM images of single XTH-2 cells.

DISCUSSION

We studied the mechanical properties of the cell cortex and cell shape of XTH-2 cells during disassembly of the microtubules using colcemid. Changes in cell shape from a fried egg shape with a concave surface between the central cell body and the thin peripheral cytoplasmic layer to a convex surface topography in this zone were accompanied by an increase in elastic stiffness. After 30 min the cell periphery starts to retract and the elastic stiffness decreases. In addition, the F-actin content increases by enhanced formation of stress fibers.

Contraction Induces Shape Changes and Stiffening of the Cytoplasm

Disruption of microtubules results in an increased tension of culture cells *(5)*, which is represented by the increase of elasticity in the cell periphery as revealed by SAM. The mechanism of this phenomena has not yet been elucidated. The explanations of the force counterbalance (and the tensegrity) model are based on the direct transfer of forces of contractile load shifting from microtubule struts to extracellular anchorage *(21,22)*. On the other hand, it has been shown that disassembly of microtubules strengthens the contractile state of the acto-myosin cytoskeleton by an increase of myosin light chain phosphorylation *(6)*.

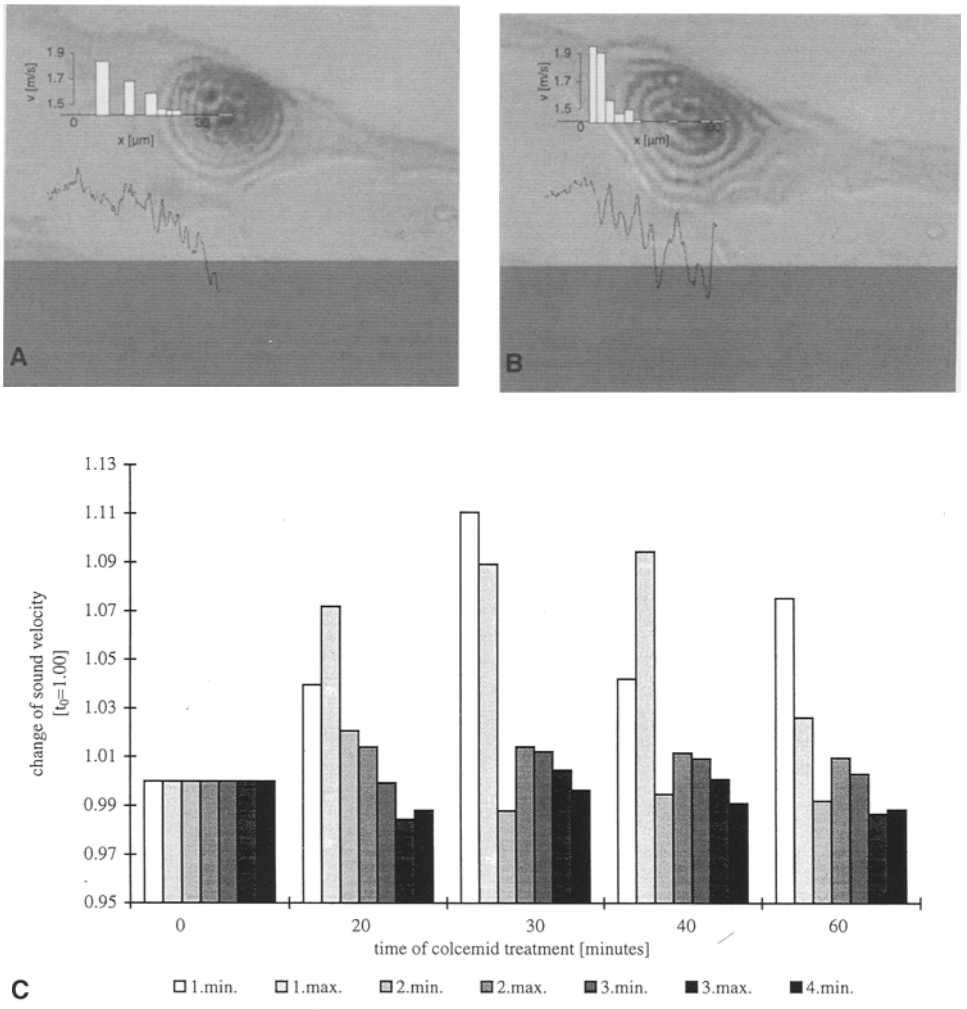

Fig. 6. Sound velocity distribution along a scanline through XTH-2 cells. Single XTH-2 cells attached to a glass cover slide were recorded using SAM. The sound velocity was evaluated in the minima and the maxima of the interference fringes according to the method of Litniewski and Bereiter-Hahn *(17)*. **(A)** An untreated XTH-2 cell. **(B)** The same cell after 60 min of colcemid treatment. The graph shows the gray levels along the scanline (x-axes of the diagram) from which the sound velocity values (bars) were calculated. **(C)** Changes of sound velocity distribution of XTH-2 cells (n = 6) during colcemid treatment. Control values were set at 1.00.

The following model for cell shape provides a relatively simple mechanistic explanation and a deeper comprehension of the process evoked by disassembly of microtubules. The shape of cells is supposed to result from:

Adhesive forces that fix the basal surface of the cell onto the substratum.

Contractile forces of the actomyosin cortex beneath the medium-facing cell membrane generate tension tangential to the cell surface, resulting in an intracellular hydrostatic pressure *(4)* and, in addition, tension between the adhesive plaques *(23)*.

We suggest that the stiffening of the cell cortex induced by enhanced contractility caused by microtubule disassembly surpasses the resistance of the cytoplasm, and the cell surface is arching, i.e., the radius of curvature in the cell body/periphery transition region flattens and the concave shape of the cell body/peripheral cytoplasmic layer is transformed to a straight or slightly convex surface. After about 30 min, when the tension force of the isometric contraction reaches its maximum, it surpasses the adhesive strength of nonfocal contact areas, the cytoplasm retracts, and thus the tension due to isometric contraction is released by isotonic contraction accompanied by a decrease in longitudinal sound velocity (elasticity).

Physiologically such a rearrangement of cytoskeletal elements inducing retraction of cytoplasm is observed during onset of mitosis. In G_2-phase, cytoplasmic microtubule disassemble *(24)* and become reorganized into the asters and the mitotic spindle. We suggest that the disassembly of microtubules in G_2-phase causes the rounding of cells at the onset of mitosis by enhancing the tension in the cytoplasm, which is no longer fully balanced by the strength of adhesion.

The longitudinal sound velocity at the cell surface never exceeds a value of 1.9 km/s, indicating that stiffening is limited by the contraction force that can be developed and by acting against the counterforces provided by the adhesive strength. The peak of elasticity after 30 min corresponds to the time with the maximal myosin light chain phosphorylation after nocodazole treatment, as determined by Kolodney and Elson *(6)*. This coincidence is in favor of the interpretation that the contractile state of the actomyosin meshwork is responsible for the stiffening of the cell surface.

Destroying microtubules disturbs not only their influence on force-generating elements, but their function in intracellular transport as well. The contribution of these fluxes, however, cannot be evaluated on the basis of the present observations.

Disruption of Microtubules Induces Reorganization of F-Actin

Simultaneous stiffening of the cytoplasm polymerization of actin and its organization into stress fibers is induced (Figs. 2B,D and 3). The fact that stress fibers become more prominent on microtubule depolymerization has been observed in a variety of specimens including *Physarum* plasmodia *(25)*, fibroblasts *(4,24)*, and density-inhibited 3T3 cells *(14)*. In dense cultures of XTH-2 cells the stress fibers originate from an area near the cell center extending to cell–cell contacts (Fig. 2B). Application of external forces, e.g., by direct stretching, induces alignment of actin filaments in the direction of tension *(26)*. Even in the absence of external forces, the actomyosin-driven contractility organizes the actin filaments (*see also* ref. *27*). Moreover, the alignment of stress fibers after disruption of microtubules indicates the direction of the actomyosin-driven contraction in dense cultures, namely, between the cell center and the cell–cell junctions. Junctional plaques are thought to play a key role in adhesion-dependent signaling *(28,29)*, and also our results revealed their significance in microtubule disassembly-induced alignment of actin fibers: In single cells the alignment of stress fibers is not as clear as in dense cultures (Fig. 2D).

The transient increase of F-actin was previously observed in 3T3 cells *(30)*. It appears to be an immediate consequence of the increase in tension because it does not require enzymatic reactions, as exemplified by cold-induced microtubule depolymerization. Furthermore, it is due to a shift in the g/F-actin equilibrium rather than evocation by induction of actin synthesis, because it takes place in the presence of cycloheximide, an inhibitor of protein synthesis (data not shown). Observations by Cooper and Pollard *(31)* support this interpretation. They were able to accelerate actin polymerization by the shearing forces occurring in a capillary viscometer. The exact mechanism of tension-stimulated actin polymerization and alignment remains to be elucidated. An alternative explanation would be the interaction of previously microtubule-associated molecules shifting g/F-actin equilibrium by binding to actin *(32)*. No decision can be made between these models at present.

Disassembly of microtubules by cold is not followed by shape changes of the cells, although the F-actin content increases. These observations raise the questions of whether contractions of the cytoplasm induced by myosin light chain phosphorylation *(6)* are reactions

subsequent to the development of tension, which may be a consequence of force imbalance brought about by microtubule depolymerization, or whether this phosphorylation is required to induce the increase in cortical tension. Comparison of cellular reactions to forces applied externally with those developed by the cells themselves provide a chance to solve this problem.

REFERENCES

1. Bray, D., Heath, J., and Moss, D. (1986) The membrane-associated "cortex" of animal cells: its structure and mechanical properties. *J. Cell Sci.* **Suppl.,** 71–88.
2. Korenstein, R., Tuvia, S., Mittelmann, L., and Levin, S. (1994) Local bending fluctuations of the cell membrane, in *Biomechanics of Active Movement and Deformation of Cells.* NATO ASI Series H42, pp. 415–423. Heidelberg, Springer Verlag.
3. Layrand, D. B., Matveeva, N. B., Teplov, V. A., and Beylina, S. J. (1972) The role of elastoosmotic parameters in locomotion of myxomycete plasmodia. *Acta Protozool.* **11,** 339–354.
4. Strohmeier, R. and Bereiter-Hahn, J. (1987) Hydrostatic pressure in epidermal cells is dependent on Ca-mediated contractions. *J. Cell Sci.* **88,** 631–640.
5. Danowski, B. (1989) Fibroblasts contractility and actin organization are stimulated by microtubule inhibitors. *J. Cell Sci.* **93,** 255–266.
6. Kolodney, M. S. and Elson, E. L. (1995) Contraction due to microtubule disruption is associated with increased phosphorylation of myosin regulatory light chain. *Proc. Natl. Acad. Sci. USA* **92,** 10,252–10,256.
7. Lüers, H., Hillman, K., Litniewski, J., and Bereiter-Hahn, J. (1992) Acoustic microscopy of cultured cells: disruption of forces and cytoskeletal elements. *Cell Biophys.* **18,** 279–293.
8. Yastas, S. and Bereiter-Hahn, J. (1996) In *International Symposium on Acoustical Imaging* **22,** in press.
9. Briggs, A. (1992) Acoustic microscopy, in *Monographs on the Physics and Chemistry of Materials* (Brook, R., Hirsch, P. B., Humphreys, C. J., and Mott, N. F., eds.), Clarendon, Oxford, UK.
10. Bereiter-Hahn, J. (1995) Probing biological cells and tissues with acoustic microscopy, in *Advances in Acoustic Microscopy* (Briggs, A., ed.), Plenum, New York, pp. 79–115.
11. Schlage, W. K., Kuhn, C., and Bereiter-Hahn, J. (1981) Established *Xenopus* tadpole heart endothelium (XTH) cells exhibiting selected properties of primary cells. *Eur. J. Cell Biol.* **24,** 342.
12. Kilmartin, J. V., Wright, B., and Milstein, C. (1982) Rat monoclonal antibodies derived by using a new nonsecreting rat cell line. *J. Cell Biol.* **93,** 173–185.

13. Faulstich, H., Trischmann, H., and Mayer, D. (1983) Preparation of tetramethylrhodaminylphalloidin and uptake of the toxin into short term cultured hepatocytes by endocytosis. *Exp. Cell Res.* **144,** 73–82.
14. Bereiter-Hahn, J. and Kajstura, J. (1987) Scanning microfluorimetric measurement of TRITC-phalloidin labelled F-actin in cultured cells: dependence of F-actin content on density of normal and transformed cells. *Histochemistry* **90,** 271–276.
15. Bereiter-Hahn, J. and Vesely, P. (1994) Measurement of cellular eslastic properties by acoustic microscopy, in *Cell Biology, A Laboratory Handbook* (Celis, J. E., ed.), Academic, San Diego, CA, pp. 15–24.
16. Hildebrand, J. A. and Rugar, D. (1984) *J. Microsc.* **134,** 245–260.
17. Litniewski, J. and Bereiter-Hahn, J. (1990) Measurements of cells in culture by scanning acoustic microscopy. *J. Microsc.* **158,** 95–107.
18. Hegner, S. and Bereiter-Hahn, J. (1992) Volume determination of adhering cells in culture by means of acoustic interferometry, in *Cell and Tissue Culture Models in Dermatological Research* (Bernd, A., Bereiter-Hahn, J., Hevert, F., and Holzmann, H., eds.), Springer Verlag, Heidelberg, pp. 58–66.
19. Wehland, J. and Weber, K. (1987) Turnover of the carboxy-terminal tyrosine of a-tubulin and means of reaching elevated levels of detyrosination in living cells. *J. Cell Sci.* **88,** 185–203.
20. Horwitz, S. B., Lothstein, L., and Manfredi, J. J. (1986) Taxol: mechanism of action and resistance. *Ann. NY Acad. Sci.* **466,** 733–744.
21. Buxbaum, R. E. and Heidemann, S. R. (1988) A thermodynamic model for force integration and microtubule assembly during axonal elongation. *J. Theor. Biol.* **134,** 379–390.
22. Ingber, D. E. (1993) Cellular tensegiety: defining new rules of biological design that govern the cytoskeleton. *J. Cell Sci.* **104,** 613–627.
23. Harris, A. K., Stopak, D., and Wild, P. (1981) Fibroblast traction as a mechanism for collagen morphogenesis. *Nature* **290,** 249–251.
24. Stolz, B. and Bereiter-Hahn, J. (1988) Calcium sensitivity of microtubules changes during the cell cycle of *Xenopus laevis* tadpole endothelial cells. *Cell Biol. Int. Rep.* **12,** 313–320.
25. Korohoda, W. and Kaystura, J. (1982) Demonstration of the significance of isometric contraction for the formation of stress fibres in chick embryo fibroblasts. *Folia Histochem. Cytochemistry* **20,** 153–156.
26. Fleischer, M. and Wohlfahrt-Bottermann, K. E. (1975) Correlation between tension force generation, fibrillogenesis and ultrastructure of cytoplasmatic actomyosin during isometric contractions of protoplasmic strands. *Cytobiology* **10,** 339–365.
27. Burridge, K., Fath, K., Kelly, T., Nickolls, G., and Turner, C. (1988) Focal adhesions: the extracellular matrix and the cytoskeleton. *Ann. Rev. Cell. Biol.* **4,** 487–525.

28. Geiger, B., Yehuda-Levenberg, S., and Bershadsky, A. D. (1995) Molecular interactions in the submembrane plaque of cell-cell and cell-matrix adhesions. *Acta Anat.* **154,** 46–62.
29. Bershadsky, A., Chausovsky, A., Becker, E., Lyubimova, A., and Geiger, B. (1996) Involvement of microtubules in the control of adhesion-dependent signal transduction. *Curr. Bio.* **6/10,** 1279–1289.
30. Kajstura, J. and Bereiter-Hahn, J. (1993) Disruption of microtubules induces formation of actin fibrils in density-inhibited 3T3 cells. *Cell Biol. Int.* **17,** 1023–1031.
31. Cooper, J. A. and Pollard, T. D. (1982) Methods to measure actin polimerization, *Methods in Enzymology* vol. 85, pp. 182–189.
32. Collings, D. A., Wasteneys, G. O., and Williamson, R. E. (1996) Actin-microtubule interactions in the alga *Nitella*: analysis of the mechanism by which microtubule depolymerization potentiates cytochalasin's effects on streaming. *Protoplasma* **191,** 178–190.